Paper No.

2511

CHARACTERIZATION OF THE PASSIVE FILM ON MILD STEEL IN CO_2 ENVIRONMENTS

Jiabin Han, David Young, and Srdjan Nešić
Institute for Corrosion and Multiphase Technology,
Department of Chemical and Biomolecular Engineering, Ohio University
342 West State Street, Athens, Ohio 45701

Akhilesh Tripathi
Rigaku Americas Corporation, The Woodlands, Texas USA 77381-5209

ABSTRACT

Passivation of the steel beneath a primary iron carbonate layer was elucidated to play a key role in the localized CO_2 corrosion of mild steel. Identification of the phases which constitute the film furthers the understanding of the localized corrosion mechanism. Scanning electron microscopy and X-ray diffraction indicated that $FeCO_3$ was initially formed under the test conditions, but it failed to passivate the surface. After most of the steel surface was covered with the $FeCO_3$ layer, passivation was observed during the spontaneous passivation tests. Surface analysis by grazing incidence X-ray diffraction indicated that an additional trace Fe_3O_4 phase, magnetite, was identified after the passivation of the coupon was complete, compared with the non-passive coupon with an exclusively $FeCO_3$ layer. The dominant phase that constituted the passive film was $FeCO_3$ (99.6%) while the Fe_3O_4 phase (0.4%) plays a key role in the passivation process. These results were confirmed using Rutherford Backscattering analysis.

Keywords: Localized corrosion, passive film, surface analysis, magnetite, iron carbonate.

INTRODUCTION

Previous research revealed the galvanic mechanism of localized CO_2 corrosion [1, 2]. The potential difference between anode (pit) and cathode (surroundings) is assumed to drive the localized corrosion propagation [1]. Further investigation discovered a passive film that can be formed under scaling conditions [2]. This causes the higher potential for the cathode surface outside the pit, but there was a disagreement on the nature of the passive film. The previous research on the H_2O-iron systems both with and without oxygen leads to the proposal that ferrous oxide or hydroxide was responsible for the passivation of the metal [3, 4]. As for the H_2O-CO_2-iron system, $FeCO_3$ was proposed as a phase

which "has the potential to form passive films" [5]. These results were based on potentiodynamic polarization sweeps.

In previous research spontaneous passivation was observed [2], which was an unperturbed process when compared with those experiments where passivation is achieved artificially by externally applying a potential or a current. Physical properties were different in spontaneous and artificial passive films. The present research project was designed to characterize the physiochemical properties of the spontaneous passive film by way of electrochemical measurement, SEM and XRD with grazing incidence. It was hoped that the understanding of the mechanism for the passivation was going to be elucidated by this research.

EXPERIMENTAL PROCEDURES

The set up was a typical three electrode electrochemical glass cell as described previously [1, 2]. Passive film was prepared at a temperature of 80 °C, 1 bar total pressure, 0.53 bar carbon dioxide pressure, 1 wt. % sodium chloride electrolyte and under stagnant conditions. The sample preparation follows the previously described procedure including electrolyte preparation, coupon finishing, passive film formation and post process treatment [1, 2]. The electrolyte solution was deaerated with carbon dioxide and heated to 80°C. The pH of the solution was adjusted to 8.0 by injection of $NaHCO_3$ powder. The electrolyte was purged with CO_2 for at least half hour in order to remove the introduced oxygen during addition of sodium bicarbonate crystals. The coupons were sequentially polished with 200, 400 and, for finishing, by 600 grit sandpaper. The coupons were cooled down by flushing with isopropanol during polishing. They were then ultrasonicated and blow dried with air. The coupons could then be immersed into the prepared solution. The spontaneous passivation was achieved when the open circuit potential increased and stabilized. The final potential was approximately 400 mV higher than the initial open circuit potential. At the end of the experiment, the coupons was taken out of the solution and washed by isopropanol until they cooled down to room temperature. Since precipitation of $NaHCO_3$ and NaCl on the coupon surface occurred during dehydration, this was avoided by rinsing by CO_2 deaerated DI water prior to flushing with isopropanol. Coupons were kept in desiccators until they were analyzed.

SURFACE ANALYSIS METHODS

SEM, XRD and GIXRD (grazing incidence XRD) were applied to characterized and identify the protective/passive film. Schemes for comparison of XRD and GIXRD are depicted in Figure 1 and Figure 2. The usual mode of data collection in XRD technique involves symmetric theta/2theta geometry wherein the angle of incidence and angle of diffraction increases continuously during the data collection. In such a mode the beam can penetrate deeper into the sample compared to GIXRD with a fixed small incidence angle. These small and large incidence angles for XRD and GIXRD are catalogued by the critical incidence angle [6].

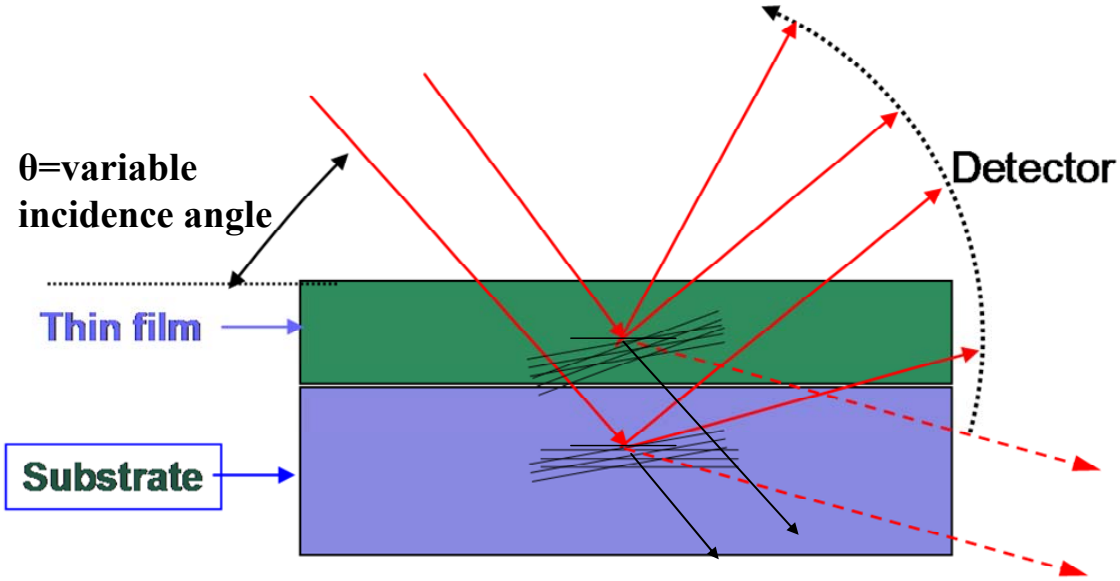

Figure 1 Scheme for XRD with larger incidence angle

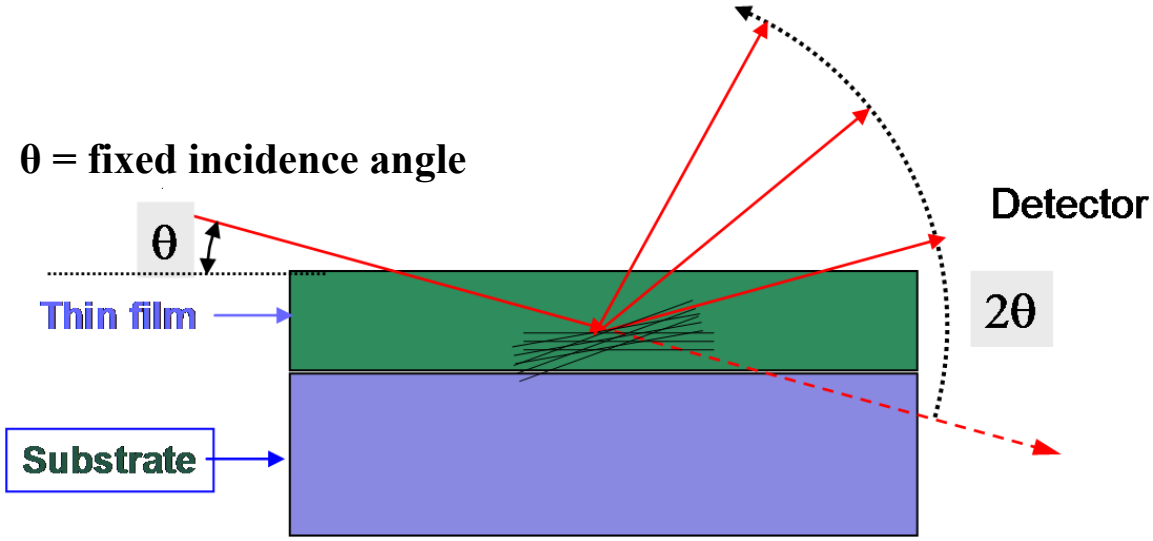

Figure 2 Scheme for XRD with grazing incidence angel (GIXRD).

RESULTS AND DISCUSSION

Geometry of the protective/passive layers by SEM

A spontaneous passivation was recorded as showed in Figure 3. The open circuit potential (OCP) was -0.775 V *vs*. saturated Ag/AgCl reference electrode immediately after the fresh coupon was immersed into the solution. The open circuit potential increased very little in the first 35 hours and it then increased to -0.416 V *vs*. saturated Ag/AgCl reference electrode, hundreds of millivolts higher than the initial OCP. This was termed as the *spontaneous passivation*, which was achieved without any externally applied potential or current in order to artificially accelerate passivation. The samples for surface analysis were taken after 0.5 hour, 12 hours and 55 hours and their surface morphology is shown in Figure 4, Figure 5 and Figure 6 respectively. The coupons in Figure 4, Figure 5 were not passivated as indicated by their low final OCP. The fact that these coupons had not become passivated was

explained by the observation that these surfaces were only partially covered by ferrous carbonate crystals. The surface shown in Figure 6 was passivated, as observed by the sharp increase of OCP from -0.776 to -0.470V *vs.* saturated Ag/AgCl reference electrode. It was also observed that the surface was almost totally covered by iron carbonate layer proving that good surface coverage is necessary before passivation can occur.

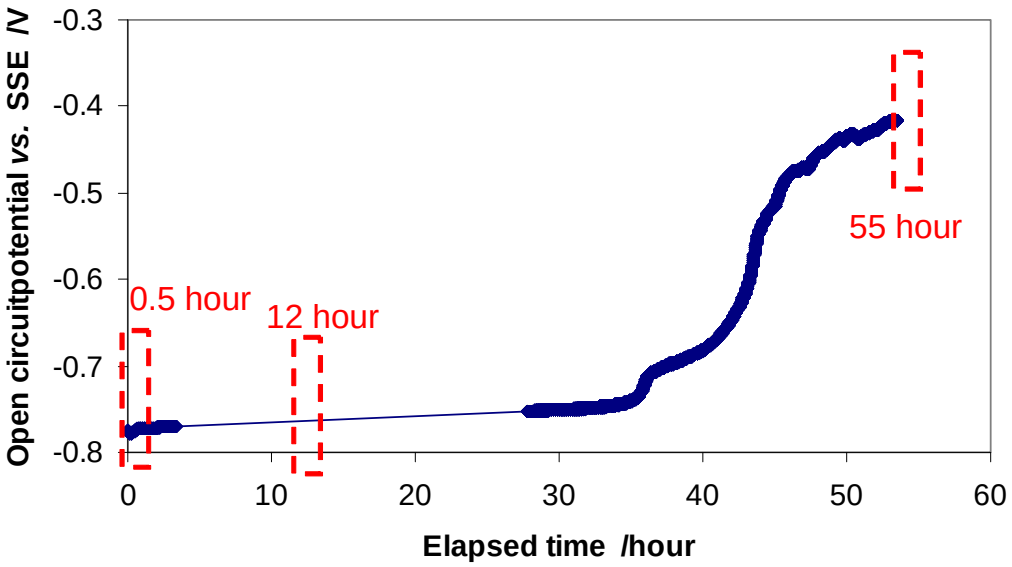

Figure 3 The OCP history for spontaneous passivation and three sample period at condition of T=80 °C, pH 7.8, NaCl=1 wt%, P_{CO2}=0.53 bar, P_{total}=1 bar, $Fe^{2+}{}_i$= 0 ppm, $\omega_{stirring\ bar}$=200 rpm.

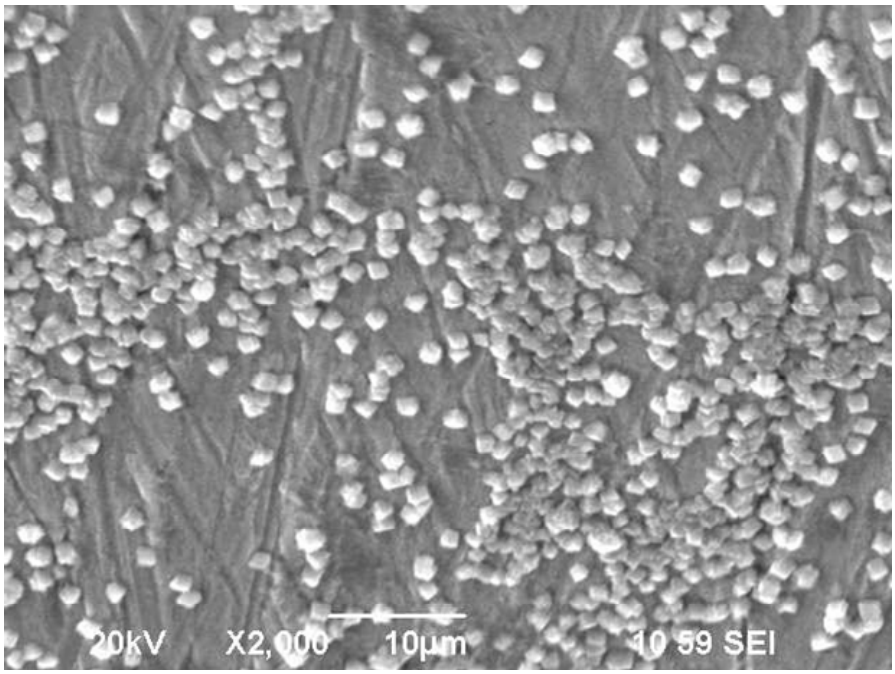

Figure 4 SEM of non-passivated coupon surface (OCP=-0.779 to -0.784 V *vs.* saturated Ag/AgCl reference electrode) after 0.5 hour immersion at T=80 °C, pH 7.8, NaCl=1 wt%, P_{CO2}=0.53 bar, P_{total}=1 bar, $Fe^{2+}{}_i$= 0 ppm, $\omega_{stirring\ bar}$=200 rpm.

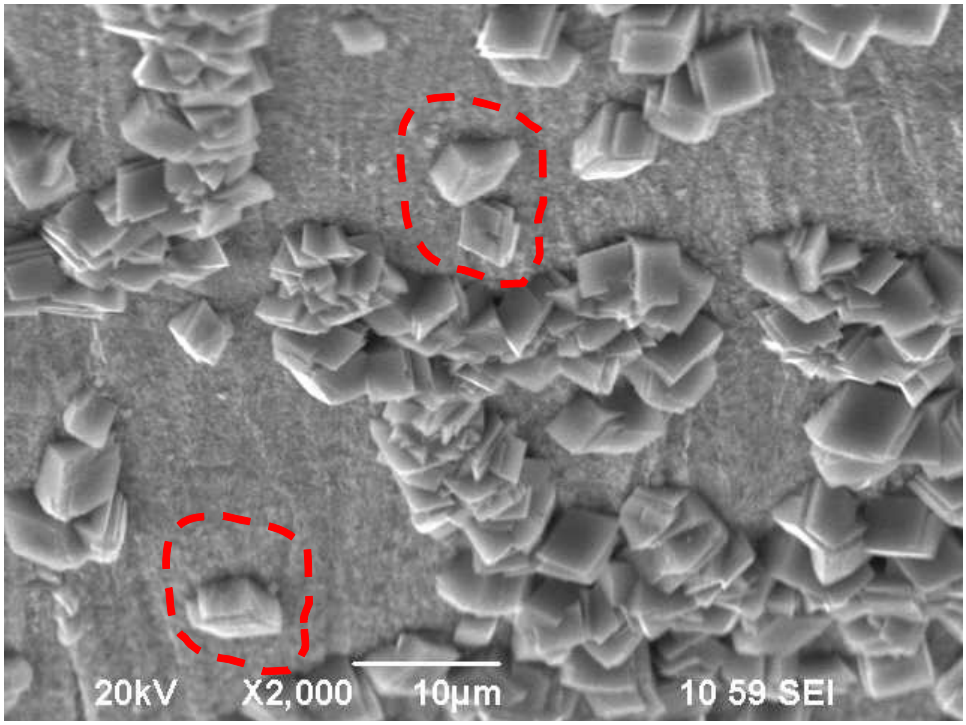

Figure 5 SEM of non-passivated coupon surface (-0.771 V to -0.782 V and then to -0.775V *vs.* saturated Ag/AgCl reference electrode) after 12 hours immersion at T=80 °C, pH 7.8, NaCl=1 wt%, P_{CO2}=0.53 bar, P_{total}=1 bar, $Fe^{2+}{}_i$= 0 ppm, $\omega_{stirring\ bar}$=200 rpm.

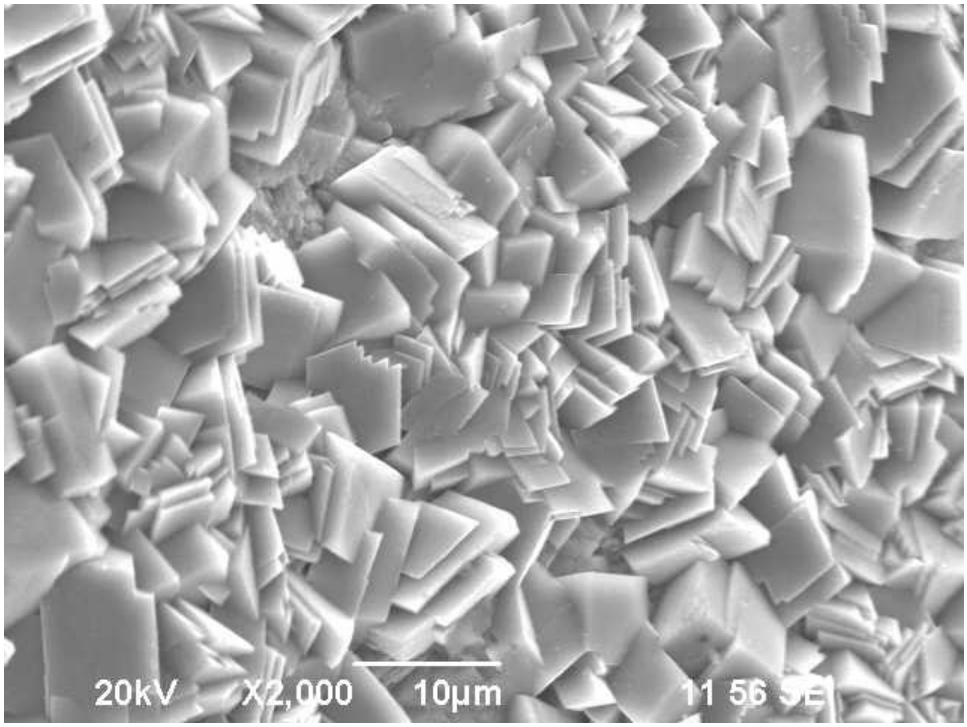

Figure 6 SEM of passivated coupon surface (-0.776 V to -0.470 V *vs.* saturated Ag/AgCl reference electrode) after 55 hours immersion at T=80 °C, pH 7.8, NaCl=1 wt%, P_{CO2}=0.53 bar, P_{total}=1 bar, $Fe^{2+}{}_i$= 0 ppm, $\omega_{stirring\ bar}$=200 rpm.

Anisotropic growth of ferrous carbonate crystal was observed in Figure 4, Figure 5 and Figure 6 after 0.5 hour, 12 hours and 55 hours. The crystals grew after their nucleation on the steel surface. From the circled morphology of the crystals in Figure 5, the crystal grew faster in the lateral direction than the perpendicular direction to the coupon surface. This phenomenon was also observed in Figure 6, where the crystals had a thin flake morphology, which proved that the growth rate was anisotropic.

Chemical composition of the passive film

The identification of the passive film is necessary since this passive film is tightly related to the spontaneous passivation. The surface analyses used in this paper were X-ray diffraction (XRD) with normal incidence and X-ray diffraction with grazing incidence (GIXRD). Two samples were obtained during a spontaneous passivation test (as depicted in Figure 7) at about 3 and 65 hours immersion, which corresponding to non-passivated surface and passive surface, respectively. The morphology of the samples before and after passivation is shown in Figure 8 and Figure 9. The morphology of the surfaces was in line with what was expected from previous observations. The surface which was partially covered by the iron carbonate layer was not passivated while passivation was achieved when a compact and dense iron carbonate layer was formed.

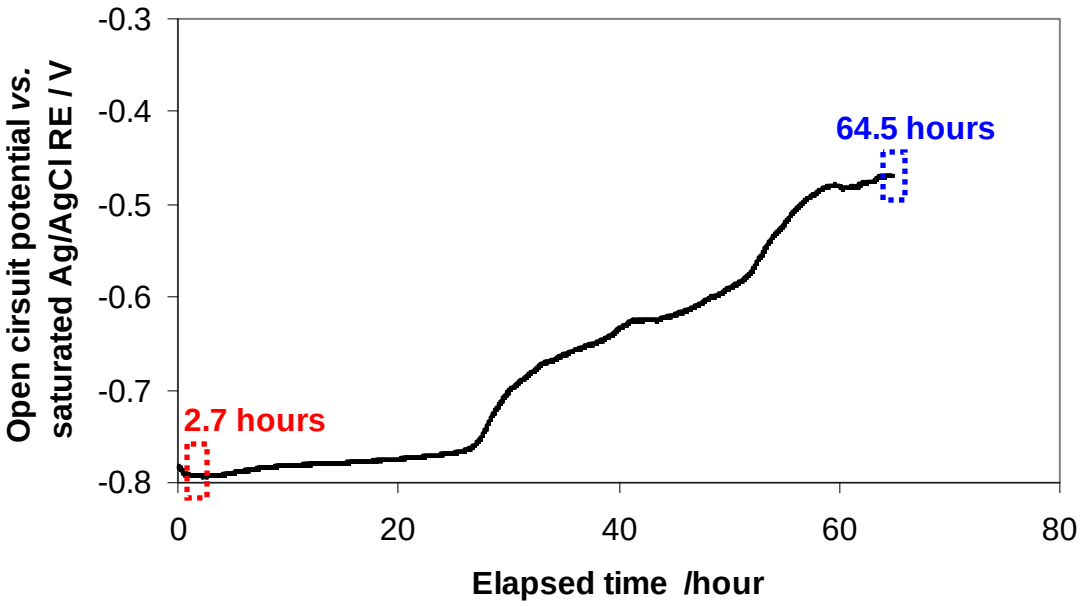

Figure 7 The OCP history for spontaneous passivation and two sample removal times under T=80 °C, pH 8.0, NaCl=1 wt%, P_{CO2}=0.53 bar, P_{total}=1 bar, $Fe^{2+}{}_i$= 0 ppm, $\omega_{stirring\ bar}$=200 rpm.

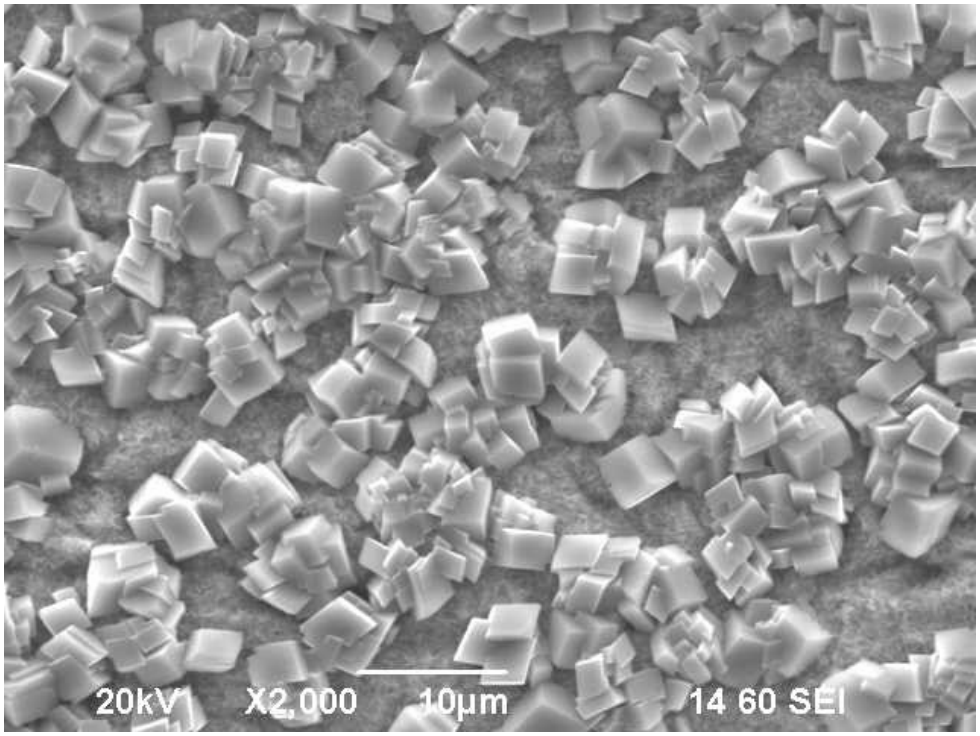

Figure 8 SEM of non-passivated coupon surface for XRD/GIXRD surface analysis (-0.777 V to -0.792 V *vs.* saturated Ag/AgCl reference electrode) after 3 hours immersion at T=80 °C, pH 8.0, NaCl=1 wt%, P_{CO2}=0.53 bar, P_{total}=1 bar, $Fe^{2+}{}_i$= 0 ppm, $\omega_{stirring\ bar}$=200 rpm.

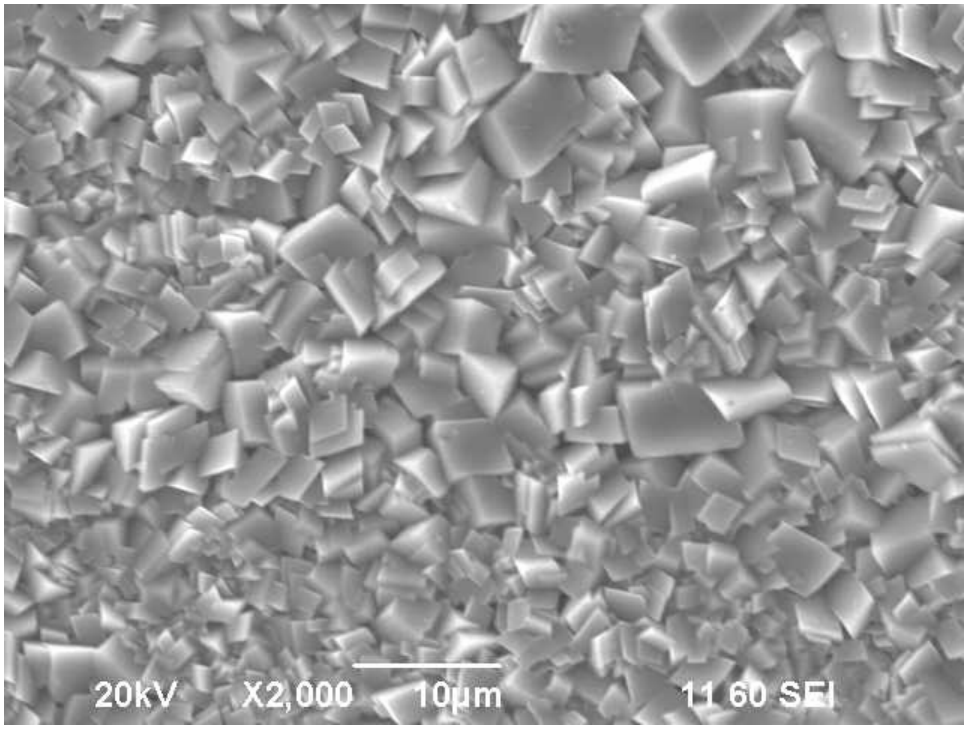

Figure 9 SEM of passivated coupon surface for XRD/GIXRD surface analysis (-0.777 V to -0.470 V *vs.* saturated Ag/AgCl reference electrode) after 64 hours immersion at T=80 °C, pH 8.0, NaCl=1 wt%, P_{CO2}=0.53 bar, P_{total}=1 bar, $Fe^{2+}{}_i$= 0 ppm, $\omega_{stirring\ bar}$=200 rpm.

Identification of the passive film using XRD: The XRD spectra with the normal incidence (a variable incidence angle and greater than the critical one) shows only the iron (substrate) and iron carbonate (layer) peaks both on samples collected before and after passivation as shown in Figure 10 and Figure 11. The passive film is usually a very thin layer approximately ten to a hundred nanometers [7]. In the θ/2θ symmetric mode, the beam penetrates deeper into the substrate steel underneath the film. Thus a weak diffraction signal from the trace amount of passive film might be masked by the dominant one from the predominant composition of iron carbonate layer and the substrate iron. Thus, XRD with grazing incidence (GIXRD) analysis was employed in order to derive maximum information from the film alone.

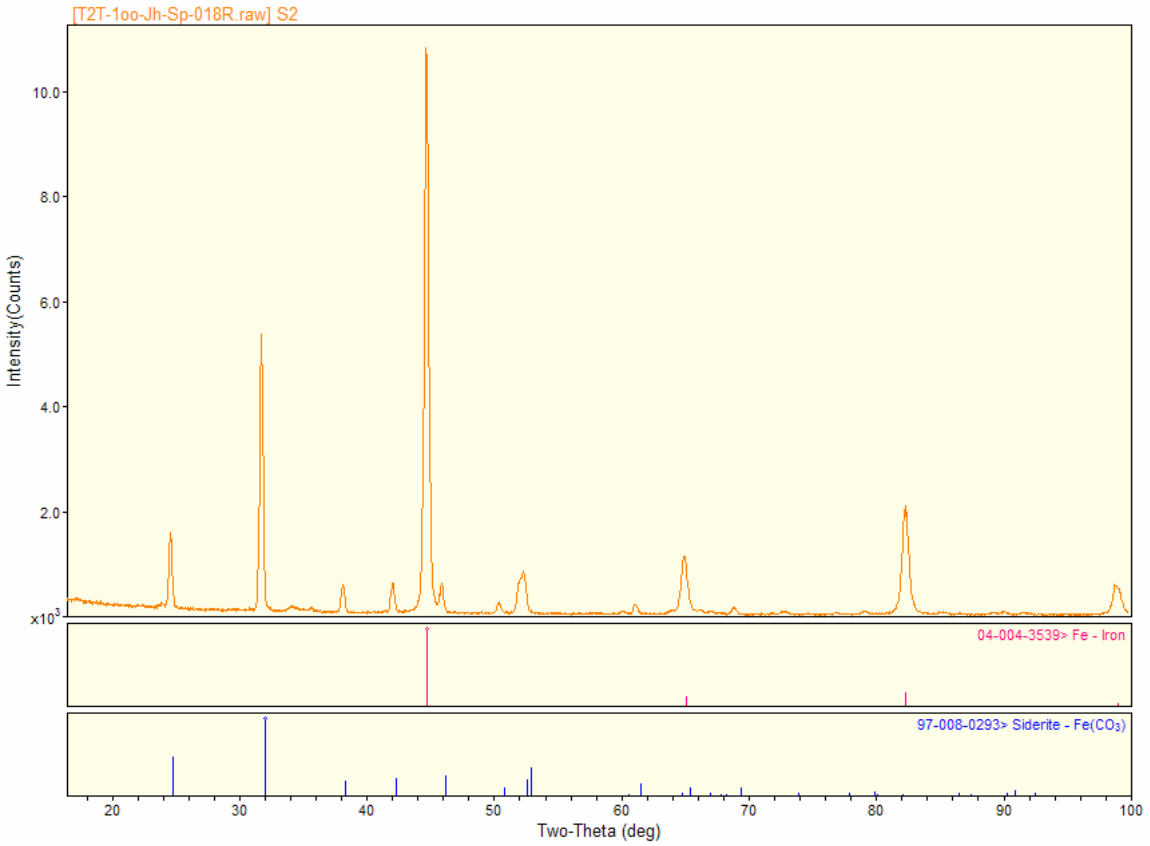

Figure 10 XRD of non-passivated coupon (-0.777 V to -0.792 V *vs.* saturated Ag/AgCl reference electrode) surface shows that only substrate Fe and $FeCO_3$ peaks were observed after 3 hours immersion at T=80 °C, pH 8.0, NaCl=1 wt%, P_{CO2}=0.53 bar, P_{total}=1 bar, $Fe^{2+}{}_i$= 0 ppm, $\omega_{stirring\ bar}$=200 rpm.

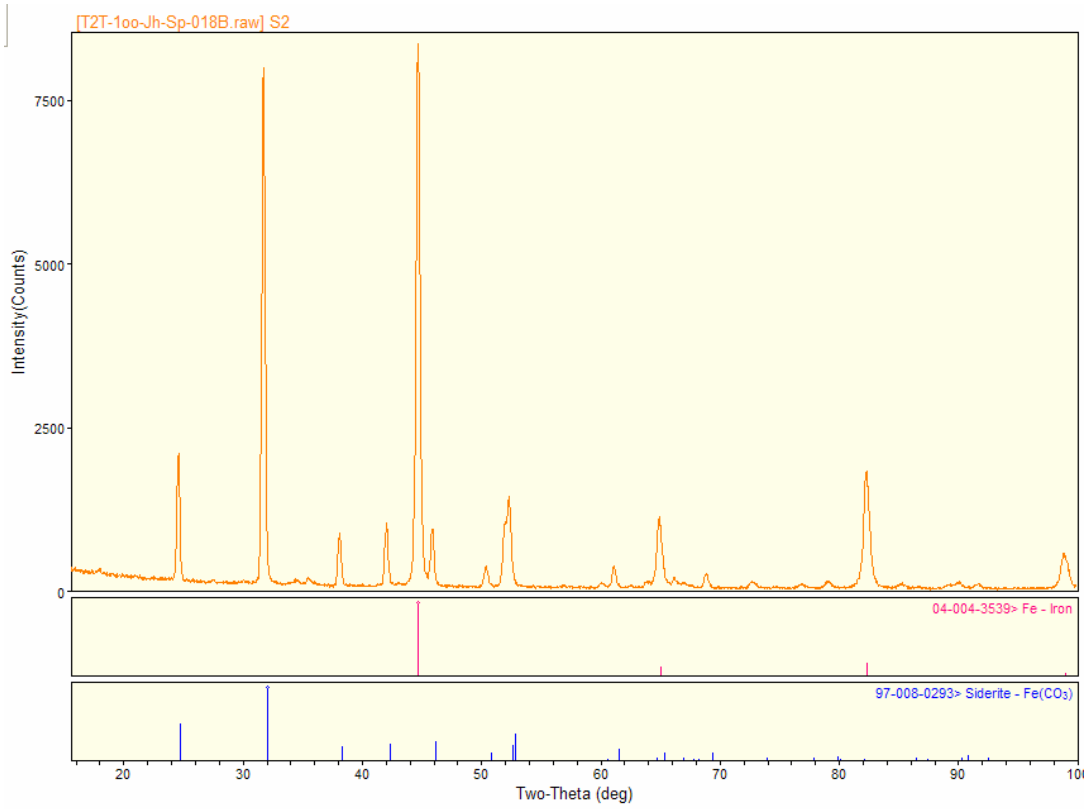

Figure 11 XRD of passivated coupon (-0.777 V to -0.470 V *vs.* saturated Ag/AgCl reference electrode) surface shows that only substrate Fe and $FeCO_3$ peaks were observed after 64 hours immersion at T=80 °C, pH 8.0, NaCl=1 wt%, P_{CO2}=0.53 bar, P_{total}=1 bar, $Fe^{2+}{}_i$= 0 ppm, $\omega_{stirring\ bar}$=200 rpm.

Identification of the passive film using XRD with grazing incidence: A GIXRD with 0.5° incidence angle was employed to get the information on the passive film. The GIXRD spectra from the sample before passivation shows only iron carbonate peaks were matched as shown in Figure 12. None of the possible phases including $Fe(OH)_2$, $Fe_2(OH)_2CO_3$, $Fe_2O_2CO_3$, $Fe_6(OH)_{12}CO_3$ and $Fe_6(OH)_{12}CO_3 \cdot H_2O$ [8, 9] were not identified, as depicted in Figure 13.

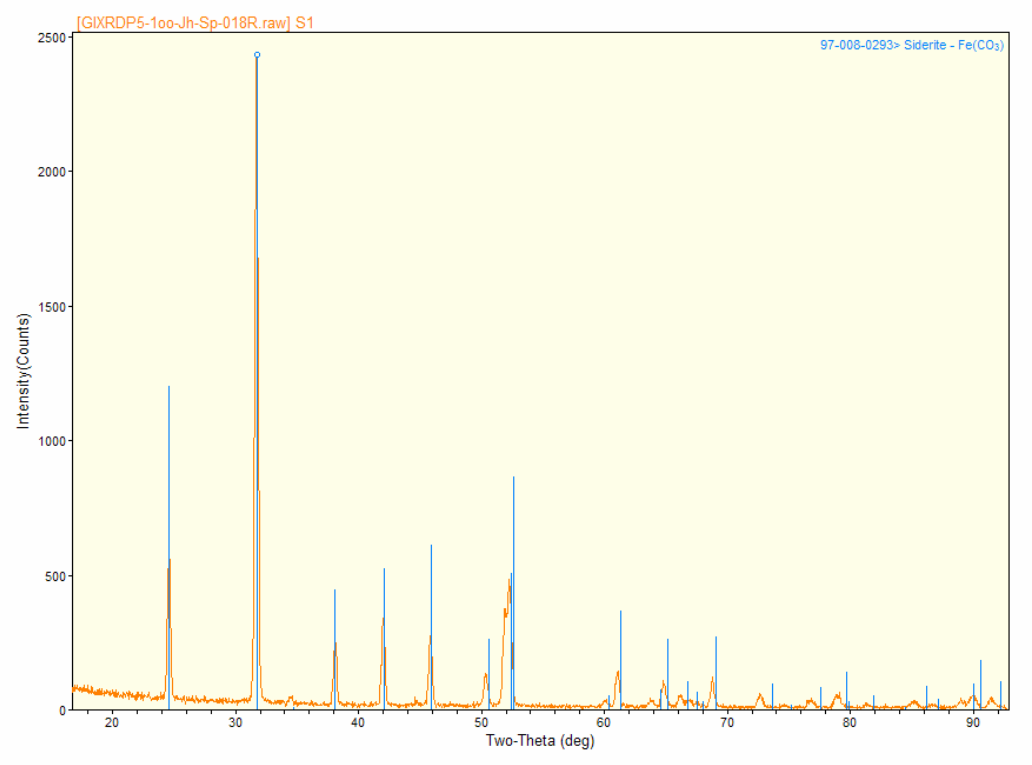

Figure 12 GIXRD of non-passivated coupon (-0.777 V to -0.792 V *vs.* saturated Ag/AgCl reference electrode) surface shows that only $FeCO_3$ peaks were observed after 3 hours immersion at T=80 °C, pH 8.0, NaCl=1 wt%, P_{CO2}=0.53 bar, P_{total}=1 bar, $Fe^{2+}{}_i$= 0 ppm, $\omega_{stirring\ bar}$=200 rpm.

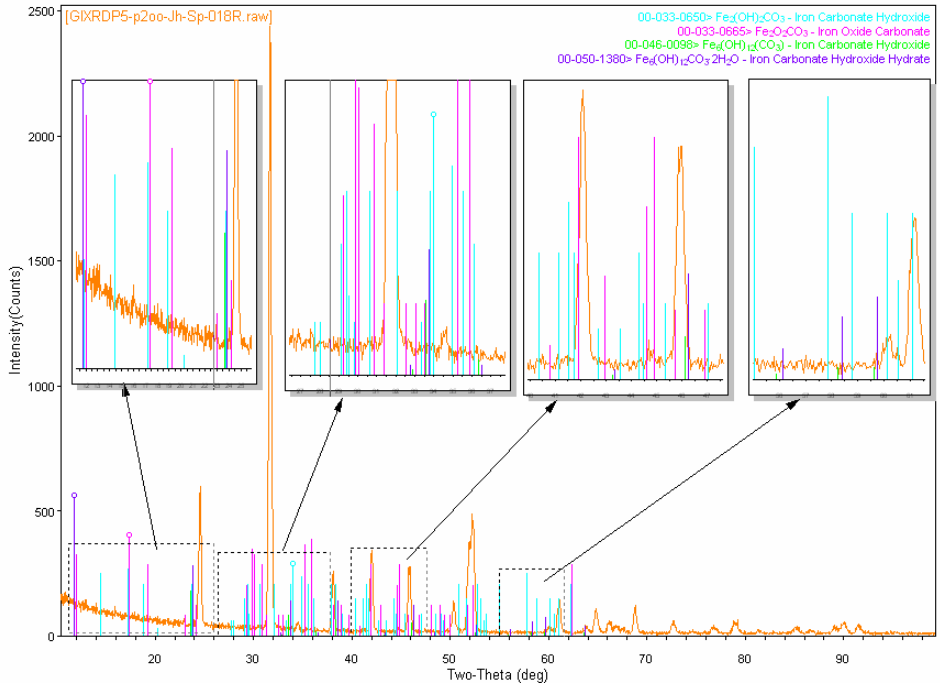

Figure 13 GIXRD of non-passivated coupon (-0.777 V to -0.792 V *vs.* saturated Ag/AgCl reference electrode) surface shows that none of the phases, $Fe(OH)_2$, $Fe_2(OH)_2CO_3$, $Fe_2O_2CO_3$, $Fe_6(OH)_{12}CO_3$, $Fe_6(OH)_{12}CO_3 \cdot H_2O$, peaks were matched after 3 hours immersion at T=80 °C, pH 8.0, NaCl=1 wt%, P_{CO2}=0.53 bar, P_{total}=1 bar, $Fe^{2+}{}_i$= 0 ppm, $\omega_{stirring\ bar}$=200 rpm.

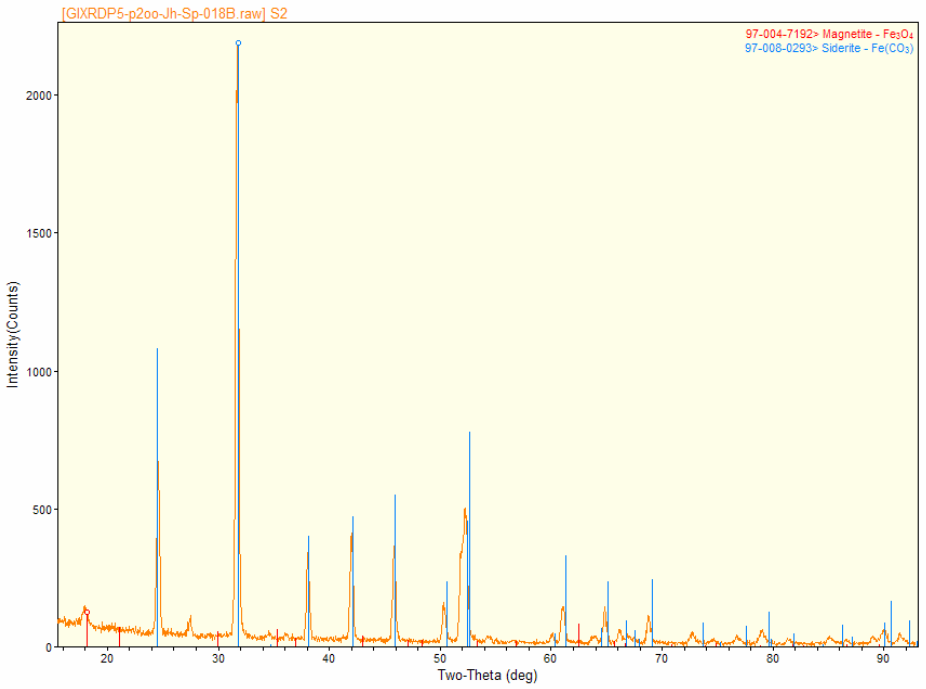

Figure 14 GIXRD of passivated coupon (-0.777 V to -0.470 V *vs.* saturated Ag/AgCl reference electrode) surface shows that only $FeCO_3$ and Fe_3O_4 peaks were observed after 64 hours immersion at T=80 °C, pH 8.0, NaCl=1 wt%, P_{CO2}=0.53 bar, P_{total}=1 bar, $Fe^{2+}{}_i$= 0 ppm, $\omega_{stirring\ bar}$=200 rpm.

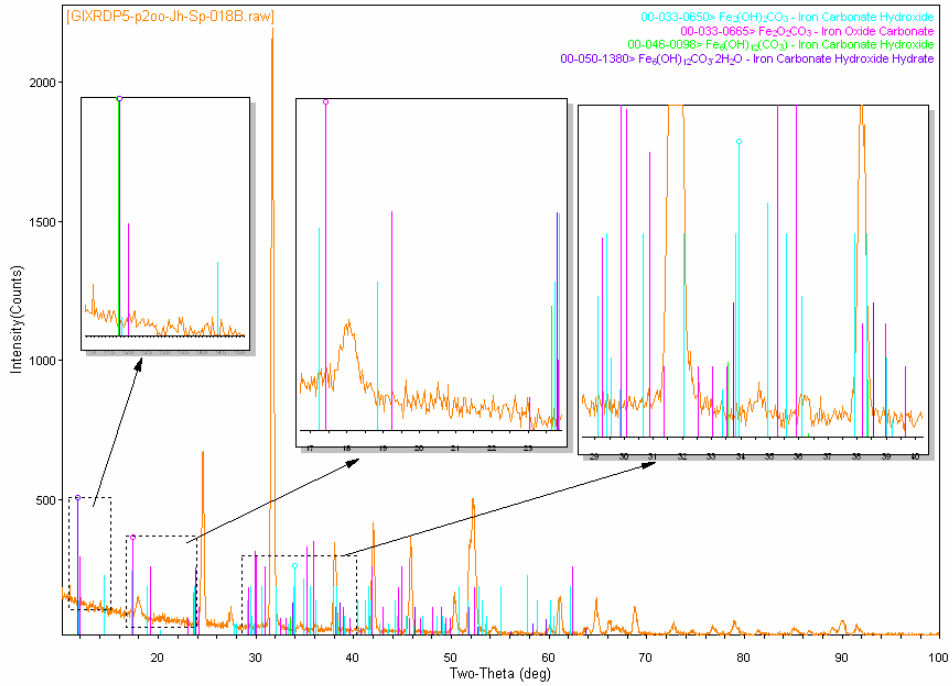

Figure 15 GIXRD of passivated coupon (-0.777 V to -0.470 V *vs.* saturated Ag/AgCl reference electrode) surface shows that none $Fe(OH)_2$, $Fe_2(OH)_2CO_3$, $Fe_2O_2CO_3$, $Fe_6(OH)_{12}CO_3$, $Fe_6(OH)_{12}CO_3 \cdot H_2O$, peaks were observed after 64 hours immersion at T=80 °C, pH 8.0, NaCl=1 wt%, P_{CO2}=0.53 bar, P_{total}=1 bar, $Fe^{2+}{}_i$= 0 ppm, $\omega_{stirring\ bar}$=200 rpm.

After the sample was passivated, Fe_3O_4 (magnetite) [10] along with the dominant $FeCO_3$ was identified by GIXRD (The observed crystalline peaks are shown in Figure 14). The other possible phases including $Fe(OH)_2$, $Fe_2(OH)_2CO_3$, $Fe_2O_2CO_3$, $Fe_6(OH)_{12}CO_3$ and $Fe_6(OH)_{12}CO_3 \cdot H_2O$ were not detected from the spectra (Figure 15). The composition of the film was quantified using the Whole Pattern Fitting module in Jade that utilizes Rietveld refinement technique [11]. A trace (0.4 wt %) amount of magnetite (Fe_3O_4) and dominant (99.6 wt %) amount of siderite ($FeCO_3$) were found as also depicted in Figure 16. From previous experience it is considered that Fe_3O_4 can be the typical composition of the thin passive film.

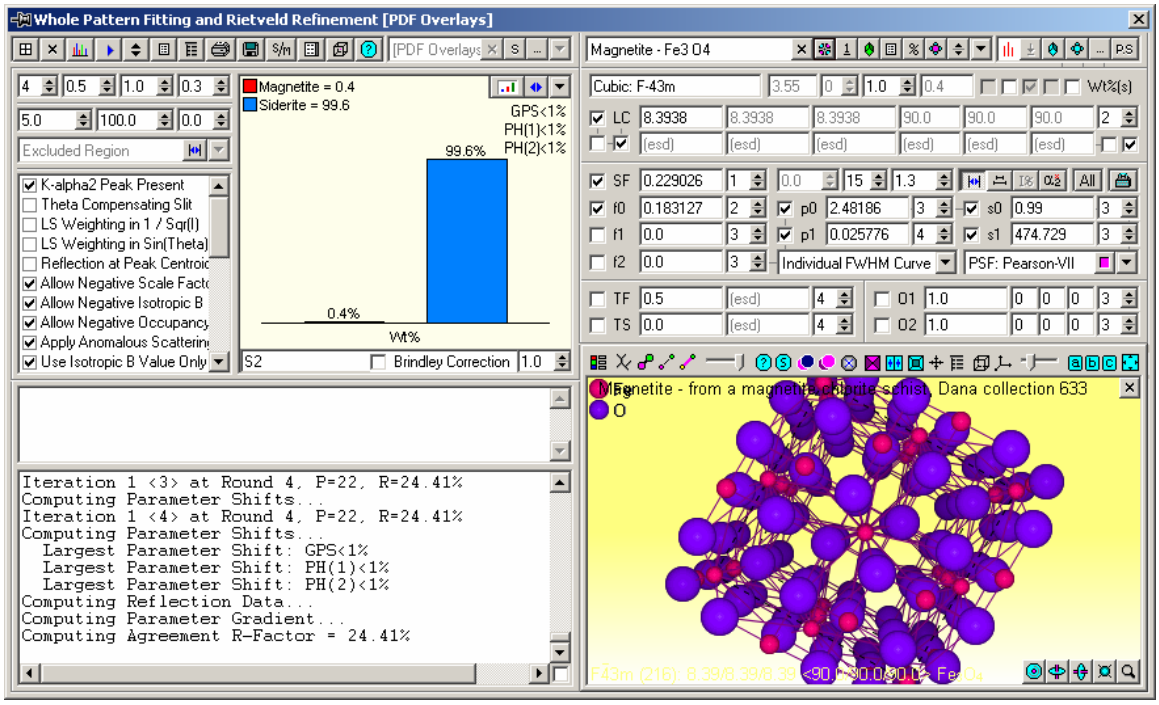

Figure 16 A Rietveld refinement window screen shot. The analysis indicated that the film in Fig 15 is composed of $FeCO_3$ 99.6 wt % and Fe_3O_4 0.4 wt % after 64 hours immersion at T=80 °C, pH 8.0, NaCl=1 wt%, P_{CO2}=0.53 bar, P_{total}=1 bar, $Fe^{2+}{}_i$= 0 ppm, $\omega_{stirring\ bar}$=200 rpm.

CONCLUSIONS

Crystalline iron carbonate formed in the first phase of the CO_2 corrosion experiments on mild steel and formed a macroscopic product layer. The secondary formed passive film was preliminarily identified to be Fe_3O_4 under the test conditions. GIXRD analysis shows only a trace amount of it (i.e. very thin passive film) which is critical to the process of passivation.

ACKNOWLEDGEMENT

The authors acknowledge the financial support from the board company members. They are Baker Petrolite, BP, Champion Technologies, Chevron, Clariant, Columbia Gas Transmission, ConocoPhillips, Eni, ExxonMobil, MI Production Chemicals, Nalco, Occidental Oil Company, Petrobras, PTTEP, Saudi Aramco, Shell, Tenaris and Total.

REFERENCES

1. J. Han, Y. Yang, B. Brown and S. Nesic, "Electrochemical Investigation of Localized CO_2 Corrosion on Mild Steel". Corrosion/2007, paper No. 07323, (Houston, TX: NACE, 2007).
2. J. Han, Y. Yang, B. Brown and S. Nešić, "Roles of Passivation and Galvanic Effects in Localized CO2 Corrosion of Mild Steel", CORROSION/2008, paper No. 08332, (Houston, TX: NACE, 2008)
3. M. Pourbaix, "Atlas of Electrochemical Equilibria in Aqueous", (English Edition), Oxford: Pergamon Press, 1966, pp. 307.
4. X. -P. Guo and Y. Tomoe, Corrosion Science, Vol. 41, 1999, pp. 1391.
5. J. K. Heuer and J. F. Stubbins, Corrosion Science, Vol. 41, 1999, pp. 1231.
6. S.A.Stepanov, "Grazing-Incidence X-Ray Diffraction", 3th Autumn School on X-ray Scattering from Surfaces and Thin Layers, Smolenice, Slovakia, October 1-4, 1997.
7. B. MacGougall and M. J. Graham, "Growth and Stability of Passive Film" (Chapter 6) in P. Marcus (Editor), "Corrosion Mechanisms in Theory and Practice", (2nd Edition), New York., USA: Marcel Dekker, Inc., 2002, pp. 190.
8. R. De Marco, Z. Jiang, B. Pejcic, and E. Poinen, Journal of The Electrochemical Society, Vol.152, No. 10, 2005, pp. B389.
9. R. De Marco, Z. Jiang, D. John, M. Sercombe and B. Kinsella, Electrochimica Acta, Vol.52, 2007, pp. 3746.
10. H. S. W. Chang, C.-C. Chiou, and Y.-W. Chen, Journal of Solid State Chemistry, Vol.128, 1997, pp. 87.
11. H.M. Rietveld. Journal of Applied Crystallography, Vol.2 (2), 1969, p. 65.